AN ANALYSIS OF THE RELAXATION OF RESIDUAL STRESSES BY USING VIBRATIONAL CONDITIONING*

K.K. WAHI, D.E. MAXWELL

Science Applications, Inc., 2450 Washington Avenue, Suite 120, San Leandro, California 94577, U.S.A.

Application of forced vibrational conditioning to anneal residual stresses in butt-welded pipes is the subject of this investigation. Numerical simulations of the butt-welding of pipes, and the subsequent modification of the residual stresses due to forced vibration are performed. The object is to evaluate the worthiness of vibrational conditioning as a possible means of relaxing residual stresses, with or without superimposed heat treatment.

Numerical simulations of various post-welding treatments following the deposition of seven passes in the butt-welding of a 4-in.-diameter pipe have been carried out using two-dimensional, explicit finite-difference techniques. The variations consist of 1) forced vibrations at the end of Pass 7 (after ambient temperatures prevail); 2) forced vibrations including a heating phase at the end of Pass 7 (after ambient temperatures prevail); 3) forced vibrations during Pass 7, vibrations started after peak temperatures are reached in the weldment; and 4) forced vibrations commencing at the beginning of Pass 7. In the present method, explicit solutions for the thermal and mechanical responses are obtained simultaneously at each increment of time. This allows one to couple the two solutions if one so desires. Additionally, material nonlinearities are incorporated efficiently and accurately.

In the context of the present work, a post-welding treatment refers to cold vibrations or vibrations with a heating phase. The forced vibrations were driven by applying a cyclic stress at the ends of the pipe to excite longitudinal vibrations. The driving frequency was chosen to be equal to the lowest natural frequency of the system defined by the numerical mesh. The peak-to-peak magnitude of the applied stress was chosen to be the yield strength at room temperature; this would ensure excursions into the plastic loading and deformation regime whether heating is part of the post-welding treatment or not. It was necessary to employ certain time-step scaling techniques to increase the size of the stable mechanical time step without compromising the essential physics.

The final residual stress fields of the various cases of post-welding treatments were evaluated with respect to the baseline case which had neither forced vibrations nor a "heat treatment". All cases, when compared to the baseline case, showed substantial annealing of the residual stresses, particularly in the inner-radius regions of the pipe where stress-induced corrosion cracking may be a consideration. The case that combined vibrations with a

*Work performed under contract to Electric Power Research Institute, Palo Alto, CA.

heating phase at the end of Pass 7 gave the best overall annealing, whereas the case of vibrating cold resulted in the least overall annealing (but the best annealing in the inner-radius region). Two major conclusions of this study are that 1) it is feasible to perform thermomechanical simulations of welding and post-welding processes that expose the detailed mechanics of annealing, and 2) the concept of using forced vibrations is not without merit, as demonstrated by the numerical analyses performed in this work, and deserves further consideration.

TABLE I. FORCED VIBRATIONS AND HEAT TREATMENT SCHEDULE

	Start time, s			Stop time, s		
Case	Compute	Vibrate	Heat Treat	Heat Treat	Vibrate	Compute
I	255	--	--	--	--	315
II	315	315	--	--	335	345
III	315	315	315	345	~349	~354
IV	255	255	--	--	305	315
V	255	~259	--	--	309	315

TABLE II. DEFLECTION PARAMETERS* D AND X, AND THEIR CHANGES

	Time, s		Dimension, cm		Change in dimension, cm
	Initial	Final	Initial	Final	
Case	t_i	t_f	D	D	ΔD
I	255	315	0.01896	0.04452	0.02557
II	315	345	0.04452	0.04642	0.00190
III	315	354	0.04452	0.06361	0.01909
IV	255	315	0.01895	0.04525	0.02631
V	255	315	0.01895	0.04580	0.02685
I + II	255	345	0.01896	0.04642	0.02746
I + III	255	354	0.01896	0.06361	0.04465
			X	X	ΔX
I	255	315	4.84885	4.83882	- 0.01003
II	315	345	4.83882	4.83912	+ 0.00030
III	315	354	4.83882	4.80890	- 0.02992
IV	255	315	4.84885	4.83809	- 0.01076
V	255	315	4.84885	4.83841	- 0.01044
I + II	255	345	4.84885	4.83913	- 0.00972
I + III	255	354	4.84885	4.80890	- 0.03995

*These parameters are defined by eqs. (2) and (3).

Summary (continued)

1. Introduction

Vibrational conditioning has been suggested as a technique to anneal residual stresses in weldments [1, 2]. Weiss [3] has performed controlled experiments on circular plates and has shown that vibrational amplitudes corresponding to about half of the yield strength provides a substantial reduction in residual stress. Unfortunately, most weldments are of a more complex geometry and the art associated with the optimum application of forced vibrations is not developed. A more complete understanding of the combined effects of geometry, yielding, creep, and behavior in the vibrational environment is required before the commercially available vibrational equipment can be properly assessed and utilized.

When complex geometries are to be analyzed or when parametric evaluations are necessary, one often resorts to numerical modeling techniques. The thermomechanical response of a multi-pass pipe weld has been simulated using numerical techniques by Wahi et al. [4] and Rybicki and Stonesifer [5], to name a few. Explicit finite-difference numerical techniques have been applied in the present study to simulate the effects of post-welding treatments, such as vibrational conditioning or heat treatment or a combination of the two, on weldments with residual stresses. These calculations are performed using the STEALTH 2-D code [6].

2. Finite-Difference Simulations

The numerical, residual stress field results of a previous study by Wahi et al. [4] on the multi-pass butt-welding of 4-inch-diameter pipe sections provide the initial conditions for the various simulations of the current study. Although all seven passes of a welding sequence were simulated in that study, the results at the start of Pass 6 were used as the restart point for the present study. This was done, in part, to ensure that minor modifications in some of the modeling techniques were exercised in arriving at the equilibrium (end of Pass 7) residual stress state prior to any vibrational conditioning. Moreover, since two of the five parametric cases considered had imposed vibrations during the heating phase of the new Pass 7, it was important to obtain a compatible set of initial conditions at the start of Pass 7. The same numerical mesh as before [4] was employed, but with a modified set of boundary conditions, as described next.

2.1 End Conditions and Forced Vibrations

The previous study employed a special constraint corresponding to no bending at the ends of the pipe. This constraint was omitted for all cases in the present study. It was felt that this would reduce the magnitude of unrealistic residual stresses near the pipe ends (as seen in the previous study) and give a more accurate description of residual stresses in the central weldment region.

The vibrations were forced by applying cyclic stress conditions, σ_{vib}, imposed at the two ends of the pipe according to eq. (1).

$$\sigma_{vib} = \pm A_o \sin[\omega(t - t_o)] \tag{1}$$

The peak amplitude, A_o, was assigned a numerical value of 100 MPa. This corresponds to one-half of the yield stress at ambient temperature, a value recommended by Weiss [3]. The parameter t refers to problem time, and t_o corresponds to the problem time at which vibrations commence. The driving frequency, ω, was chosen to be 1.5708 rad/s and was approximately equal to the lowest natural frequency of the finite-difference mesh. The mechanical frequencies are on a pseudo scale in these simulations. However, the response that develops is realistic with respect to the number of oscillations.

2.2 Other Modeling Aspects

Except for the modifications discussed below, all the modeling techniques of [4] were employed as before.

The uniform density scaling technique was replaced by a Pseudo-Time step Scaling (PTS) method that is superior to the old method. The object in either method is to obtain comparable mechanical and thermal time steps. Although the PTS method does not scale density per se, it essentially finds an optimum scale factor for each cell in lieu of a constant scale factor for the entire mesh [7].

When explicit finite-difference codes are used to model quasi-static or quasi-dynamic systems, it is necessary to use dynamic relaxation or damping in order to maintain a near-equilibrium stress condition. This method allows for near-critical damping of the lowest natural frequency and provides attenuation of the higher frequencies introduced in the basic difference equations.

2.3 Parametric Cases of Post-Welding Treatments

Five different simulations were made, of which four included some form of post-welding treatment. These cases are summarized in Table I. A reference time of 255 seconds corresponds to the start of Pass 7.

The prescribed heat treatment of Case III was modeled by a heat source applied uniformly across the mesh, followed by a corresponding heat sink. Figure 1 shows the mesh configuration at t equal to 315 seconds for the baseline case. Also shown is the (I,J) index labeling scheme that will be used to identify various locations in the remainder of this paper. To summarize the thermal boundary conditions, note that the inner and outer pipe surfaces (at $J = 1$ and $J = 11$) have convective and radiative losses, whereas the two ends (at $I = 1$ and $I = 35$) are isothermal at an ambient temperature of 293.16 K. The Pass 7 welding bead is comprised of six cells, bounded by $I = 15$ to 18 and $J = 9$ to 11 (see Figure 1). The cooling rate was enhanced artificially by introducing a prescribed heat sink at 285 seconds in Case I (baseline) and at 320 seconds in Case III. The heat sink was applied such that proper temperature gradient directions were maintained. In the present study, heat was extracted more slowly than in the previous study [4] to insure that at least five vibrational cycles would be experienced during heat extraction.

3. Results and Comparisons

3.1 Deflections

If examined carefully, Figure 1 shows that the inner pipe surface in the weldment region is warped inwards with respect to the pipe ends. The difference in shape before and after vibrational conditioning corresponds to a conversion of locked stresses into plastic strains, and provides a qualitative measure of annealing. Let R_ℓ, R_c, and R_r be the inner pipe radii at the left end, the right end, and the center. Now define parameter D by eq. (2), and parameter X by eq. (3). These parameters provide measures of warping and mean inner surface radius.

$$D = (R_\ell + R_r)/2 - R_c \tag{2}$$

$$X = (R_\ell + R_r + 2R_c)/4 \tag{3}$$

Table II provides values of D, X, ΔD, and ΔX for the various cases. Using deflection as a criterion, Table II indicates that Case III gives the best annealing and Cases II, IV, and V provide virtually the same amount of annealing.

3.2 Residual Total Stress Fields

The residual radial stresses were an order of magnitude lower than the longitudinal or the hoop stresses, and need not be discussed further.

Figure 2 compares the final longitudinal stress fields for all five cases. Let us focus our attention on the middle third of the pipe length, for it is believed that the end effects would be negligible in a longer pipe. The longitudinal stresses are tensile (positive) near the inner surface and compressive near the outer surface for all cases. The peak contours are ± 200 MPa for Case I, but are only ± 50 MPa for Cases II through V. This indicates a substantial annealing effect of the longitudinal stress component. The area encompassed by the peak contours is less for Case II than for the other cases. Using the longitudinal residual stress criterion, therefore, Case II appears to provide the best annealing. Cases III, IV, and V rank closely behind Case II.

The residual hoop stress contours are displayed in Figure 3 for all cases. The peak contour for Case I is 150 MPa and is located near the inner surface. Case II has a peak contour of 100 MPa, with its center having migrated radially to mid-thickness. In Cases III, IV, and V, the peak contour is also near the mid-thickness, but its magnitude is only 50 MPa. The area encompassed by the 50 MPa contour is the smallest for Case III, corresponding to the most annealing of the hoop stress. Cases IV and V rank second, and Case II exhibits the least amount of annealing.

In summary, the baseline residual stresses (longitudinal and hoop) have peak values near the yield stress. These peak values are reduced to about one-third of the yield stress in all cases except one -- the hoop stress is reduced to only two-thirds of the baseline hoop stress in Case II.

3.3 Residual Deviatoric Stress Fields

According to the von Mises yield criterion, plastic flow (essential for annealing) occurs when the equivalent stress, σ_e, equals the yield strength, Y. For the two-dimensional axisymmetric case, σ is defined by eq. (4); and it is also equal to $\sqrt{3J_2}$ where J_2 is the second invariant of the stress deviator tensor.

$$\sigma_e = \left\{\frac{1}{2}\left[(\sigma_r - \sigma_\theta)^2 + (\sigma_\theta - \sigma_z)^2 + (\sigma_z - \sigma_r)^2\right] + \tau_{rz}^2\right\}^{\frac{1}{2}} = \sqrt{3J_2} \qquad (4)$$

In eq. (4), σ_r, σ_θ, and σ_z are the radial, hoop, and longitudinal stresses, respectively, and τ_{rz} is the shear stress. It is convenient to represent the proximity to the yield surface by a yield factor, YF, which is defined by the ratio $Y/\sqrt{3J_2}$. When YF equals unity, plastic flow is indicated. Values greater than one measure a "safety factor" with respect to avoiding the plastic flow. It is hoped that after a post-welding treatment, YF has a value much greater than one.

The contours of residual YF for the five cases are displayed in Figure 4. As before, let us focus our attention on the central third of the pipe length. The YF contour levels for Case I have three intermediate values between YF = 1 and YF = 2, namely, 1.125, 1.25, and 1.5. Large regions of the mesh have a YF value of less than 1.5, indicating large deviatoric stresses on the verge of triggering plastic flow. The low values of YF along an inner surface suggest a potential problem with respect to corrosive cracking. The minimum values of YF for other cases ranged between 1.7 and 1.8, and they occurred near the outer surface at the tip of the weldment. Table III gives the maximum and minimum values of YF along the

inner surface in the central inch of pipe length. Using YF as a measure of the amount of annealing, substantial annealing is observed in Cases II through V.

The forced vibrations caused stress excursions into the plastic domain. The plastic flow was largest in regions with large initial values of $\sqrt{3J_2}$ since these regions encountered the yield surface first. The elastic deviatoric load then shifted to the remaining elastic regions, sometimes enhancing their values of $\sqrt{3J_2}$ and contributing to their subsequent plastic flow. The average effect was a substantial reduction in the final equilibrium values of $\sqrt{3J_2}$, particularly in regions with high initial values.

The driving stress applied to the pipe ends for all cases was $\pm$ 100 $\sin[2\pi(t - t_0)/4]$ MPa. The Case II time history of σ_z for the zone I = 33, J = 11 is displayed in Figure 5 and is typical of all cases. The driving stress for Case II was imposed at 315 seconds and terminated at 335 seconds. Final equilibrium was reached in about two more oscillations, i.e., 8 seconds more of problem time following the termination of forced vibrations.

4. Summary and Conclusions

The annealing cases of this study employed half of the yield stress at ambient temperature at the pipe ends to drive longitudinal vibrations during the different heat histories of Cases II through V. The residual stress results were compared to those of Case I, the baseline case without forced vibrations. All annealing cases showed substantial reductions of residual stress, particularly in the inner radius regions of the pipe where stress-induced corrosive cracking is a consideration. Case III, with its post-weld heat treatment, gave the best overall annealing. Case II, with cold vibrations, gave the least overall annealing, but the best annealing in the inner radius region. The results of Cases IV and V, with vibrations during welding as well as weld cooling, were similar and were intermediate between Cases II and III with respect to annealing.

Even though no case with a different peak amplitude for the applied oscillatory stress was modeled, the observed annealing mechanisms suggest that the ranking of Cases II through V would not change with respect to annealing. There were no cases with an applied radial stress to drive the vibrations and it is not known how that might influence the effectiveness of various annealing cases. The current study did not use work hardening or a creep model. Creep should further reduce the deviatoric stresses. The effect of work hardening is not as obvious. Both effects would require more oscillations for proper simulation and would increase computer costs. This study demonstrates that new computing techniques are available to expose the detailed mechanisms of annealing in practical cases.

References

[1] CHEEVER, D., ROWLANDS, E., "Vibrational Conditioning of Castings and Weldments: An Exploratory Study," Conf. on Control of Distortion and Residual Stress in Weldments, Chicago, Illinois (USA), November 16-17, 1976.

[2] MADSEN, O., "Practical Uses of Vibrational Conditioning," Conf. on Control of Distortion and Residual Stress in Weldments, Chicago, Illinois (USA), November 16-17, 1976.

[3] WEISS, S., "Analysis of Vibrational Stress Relieving," Conf. on Control of Distortion and Residual Stress in Weldments, Chicago, Illinois (USA), November 16-17, 1976.

[4] WAHI, K., et al., "Finite-Difference Simulation of a Multi-Pass Pipe Weld," Fourth Intl. Conf. on Structural Mechanics in Reactor Technology, San Francisco, California (USA), August 15-19, 1977.

[5] RYBICKI, E., STONESIFER, R., "Computation of Residual Stresses Due to Multipass Welds in Piping Systems," presented at the Joint ASME/CSME Pressure Vessel & Piping Conf., Montreal, Canada, 78-PVP-104, June 25-30, 1978.

[6] HOFMANN, R., "STEALTH, A Lagrange Explicit Finite-Difference Code for Solids, Structural, and Thermohydraulic Analysis," EPRI NP-260, Vols. 1, 2, and 3, prepared by Science Applications, Inc., Oakland, California for Electric Power Research Institute, Palo Alto, California, August 1976.

[7] MAXWELL, D. et al., "An Optimization Study of the Explicit Finite-Difference Method for Quasi-Static Thermomechanical Simulations," Y/OWI/SUB-78/16549/3 (SAI-FR-821-3), Science Applications, Inc., Oakland, California. Final report prepared for Office of Waste Isolation, Union Carbide Corporation, Oak Ridge, Tennessee, March 1978.

TABLE III. MINIMUM AND MAXIMUM VALUES OF YF ALONG THE CENTRAL INCH NEAR THE INNER SURFACE

Case	Minimum	Maximum
I	1.10	1.24
II	3.9	6.9
III	2.7	4.9
IV	2.5	5.5
V	2.8	4.6

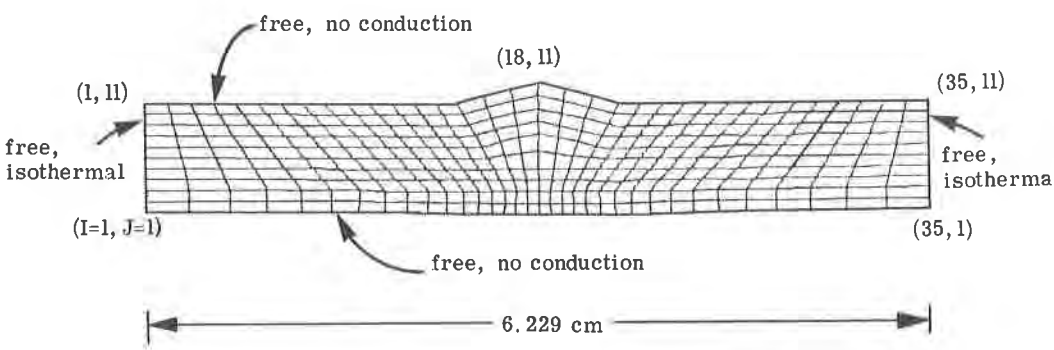

Initial Pipe Length = 6.240 cm

Initial Inner Radius = 4.859 cm

Initial Outer Radius = 5.715 cm

Figure 1. Finite-difference mesh configuration at the end of Pass 7, Case I.

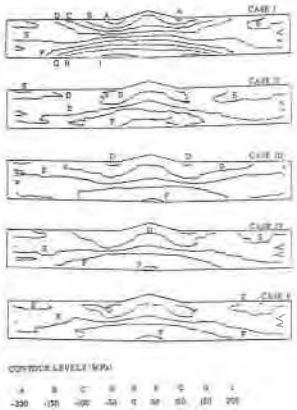

Figure 2. Contours of residual longitudinal stress, σ_z at final time, Cases I through V.

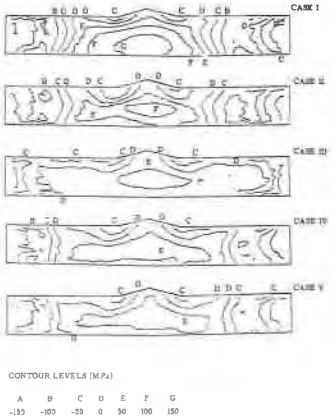

Figure 3. Contours of residual circumferential stress, σ_θ at final time, Cases I through V.

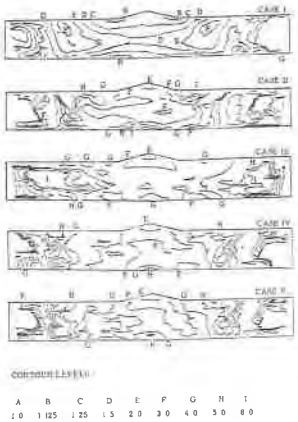

Figure 4. Contours of residual yield factor, YF at final time, Cases I through V.

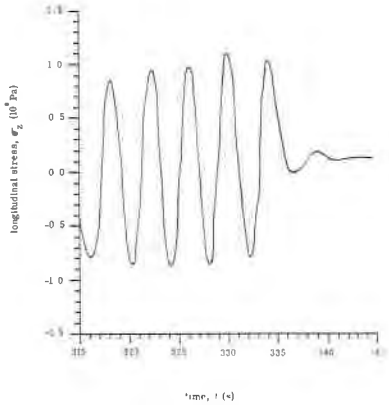

Figure 5. Time history of longitudinal stress, σ_z near the right end of pipe, Case II.